Acta Geochim (2017) 36(3):440–445
DOI 10.1007/s11631-017-0186-y

ORIGINAL ARTICLE

Distribution of rare earth elements of granitic regolith under the influence of climate

Hairuo Mao[1,2] · Congqiang Liu[1] · Zhiqi Zhao[1] · Junxiong Yang[1,2]

Received: 14 April 2017 / Revised: 21 May 2017 / Accepted: 7 June 2017 / Published online: 23 October 2017

Abstract The distribution and anomalies of rare earth elements (REEs) of granitic regolith were studied in Inner Mongolia and Hainan Island, China. One profile showed slight REE enrichment of an upper layer and no obvious light REE/heavy REE (LREE/HREE) fractionation (La_N/Yb_N of 0.9). The second profile was significantly enriched in REEs and enriched in LREEs in the upper portion ($La_N/Yb_N > 1.8$). Eu, Ce, and Gd anomalies of the two profiles are different. Slightly negative Eu, Ce, and Gd anomalies in NMG-3-1 indicate slow dissolution of primary minerals and little secondary products; in contrast, a positive Eu anomaly in HN-2 suggests the vegetation cycle may contribute to soil. The Ce anomaly of HN-2 reflects oxidation of Ce and coprecipitation by Fe- and Mn-oxides and organic matter. Correlation between Ce and Gd anomalies in HN-2 suggests Ce and Gd are both influenced by redox-reduction.

Keywords Rare earth elements · Granitic regolith · Weathering · Ce anomaly · Eu anomaly

1 Introduction

Rare earth elements (REEs) behave geochemically coherently due to systematic variations in their ionic charge to radius ratio (Henderson 1984). During chemical weathering of rocks, the behavior of REEs is mainly controlled by dissolution of primary minerals, and adsorption on clay minerals, Fe- and Mn-oxides, and organic matter (Laveuf and Cornu 2009). After release from primary minerals, REEs are either removed from the profile by soil solution or incorporated into secondary minerals, and probably transferred in the illuvial horizon. These processes lead to internal fractionation and anomalies related to REEs or to change of oxidation states for Ce. Therefore, REE distribution patterns and anomalies normalized to bedrock provide useful weathering tracers (Laveuf and Cornu 2009; Vermeire et al. 2016). The distribution of REEs during chemical weathering of igneous rock has received considerable attention (Aubert et al. 2001; Ma et al. 2007; Bao and Zhao 2008; Yusoff et al. 2013; Babechuk et al. 2014; Vermeire et al. 2016), but the influences of different climates on REEs during weathering are still not well understood. We investigated light and heavy REE (LREE and HREE) distribution and anomalies in two granitic profiles under different climates.

2 Study area

The profile NMG-3-1 is developed on monzonitic granites covered by fine black soil in Inner Mongolia, northeastern China (49°53′1.68″ N, 124°14′55.38″ E). It is in the semi-humid monsoon climatic zone. The mean annual temperature is −2.7 to −0.8 °C and mean annual precipitation is 460–490 mm. The maximum monthly temperature is 18 °C in July. NMG-3-1 is exposed by road-cut at the

11th International Symposium on Geochemistry of the Earth's Surface.

✉ Congqiang Liu
liucongqiang@vip.skleg.cn

✉ Zhiqi Zhao
zhaozhiqi@vip.skleg.cn

[1] State Key Laboratory of Environmental Geochemistry, Institute of Geochemistry, Chinese Academy of Sciences, Guiyang 550002, China

[2] University of Chinese Academy of Sciences, Beijing 100049, China

bottom of a hill covered by well-developed plants (mainly Quercus mongolica).

The profile HN-2 is developed on monzonitic granites covered by laterite in Ledong county, Hainan province, South China (9°07′14.78″ N, 18°37′51.96″ E). This region is in the tropical humid monsoon zone, controlled by the East Asian monsoon. The mean annual temperature is 24 °C. Maximum monthly temperatures of 30–32 °C occur in July and August. Annual precipitation varies from 800 to 2500 mm but averages around 1600 mm, with most precipitation occurring in the warm season. The profile is in a gentle hill covered by evergreen broad-leaved forest 500 meters northeast of Leguang Farm.

3 Results

To investigate the behavior of REEs during chemical weathering, REE distribution patterns were normalized to bedrock (granite) and to upper continental crust (UCC) (Rudnick and Gao 2003) (Fig. 1). In NMG-3-1, ∑REE varied from 95.9 to 275.7 ppm, with an average of 152.5 ppm, and ∑LREE/∑HREE varied from 10.7 to 18.5, with an average of 14.2. The ∑REE and ∑LREE/∑HREE of bedrock were 108.9 ppm and 13.6, respectively. $(La/Yb)_N$—a ratio normalized to bedrock—ranged from 0.6 to 1.4, with an average of 0.9. REE distribution patterns normalized to UCC in NMG-3-1 and HN-2 are distinct: Eu, Ce, and Gd anomalies in profile NMG-3-1 were slight, whereas HN-2 showed negative Eu anomalies, variable Ce anomalies, and no obvious Gd anomalies. REEs were enriched in the upper profile relative to bedrock and similar to bedrock in the lower profile (Fig. 1). In addition, most samples' LREEs and HREEs had no obvious fractionation during weathering. In profile HN-2, the ∑REE varied from 168.5 to 526.0 ppm, with an average of 386.8 ppm, and ∑LREE/∑HREE varied from 8.0 to 15.2, with an average of 11.5. The ∑REE and ∑LREE/∑HREE of bedrock were 71.7 and 7.7 ppm, respectively; $(La/Yb)_N$ ranged from 1.4 to 2.1, with an average of 1.8. The REE values of the entire HN-2 profile were higher than those of bedrock, and REEs were more enriched in the upper layer of the profile than in the lower. Enrichment of LREEs was observed and ∑LREE/∑HREE decreased from 10 to 200 cm (eluvial horizon).

The degree of chemical weathering of igneous rock is established by chemical index of alteration (CIA). Except for the top soil samples, CIA values in profile HN-2 increased from bottom to top of the profile (Fig. 2e); profile NMG-3-1 showed a similar trend of CIA (Fig. 2a). Eu, Ce, and Gd anomalies were determined as $Eu/Eu^* = Eu_N/(Sm_N \times Gd_N)^{1/2}$, $Ce/Ce^* = Ce_N/(La_N \times Pr_N)^{1/2}$, and $Gd/Gd^* = 3Gd_N/(Sm_N + 2Tb_N)$, respectively, where N refers to the granite-normalized value.

In profile NMG-3-1, slight Eu anomalies (from 0.8 to 1.2) were evident (Fig. 2b–d). However, the Eu/Eu* values generally increased with depth, which is opposite to the trend of CIA. Most samples exhibited a slightly positive Ce anomaly. In contrast, most samples displayed no clear Gd anomaly (Gd/Gd* ranging from 0.85 to 1.09). In profile HN-2 (Fig. 2f–h), samples exhibited a strong positive Eu anomaly (Eu/Eu* > 2) and Eu/Eu* decreased with depth, similar to CIA. In HN-2, Ce/Ce* and Gd/Gd* showed similar patterns in that Ce and Gd anomalies decreased from 10 to 200 cm and Ce and Gd anomalies of samples below 200 cm oscillated slightly. A positive Ce anomaly was observed in most samples, whereas nearly all samples had no significant Gd anomaly.

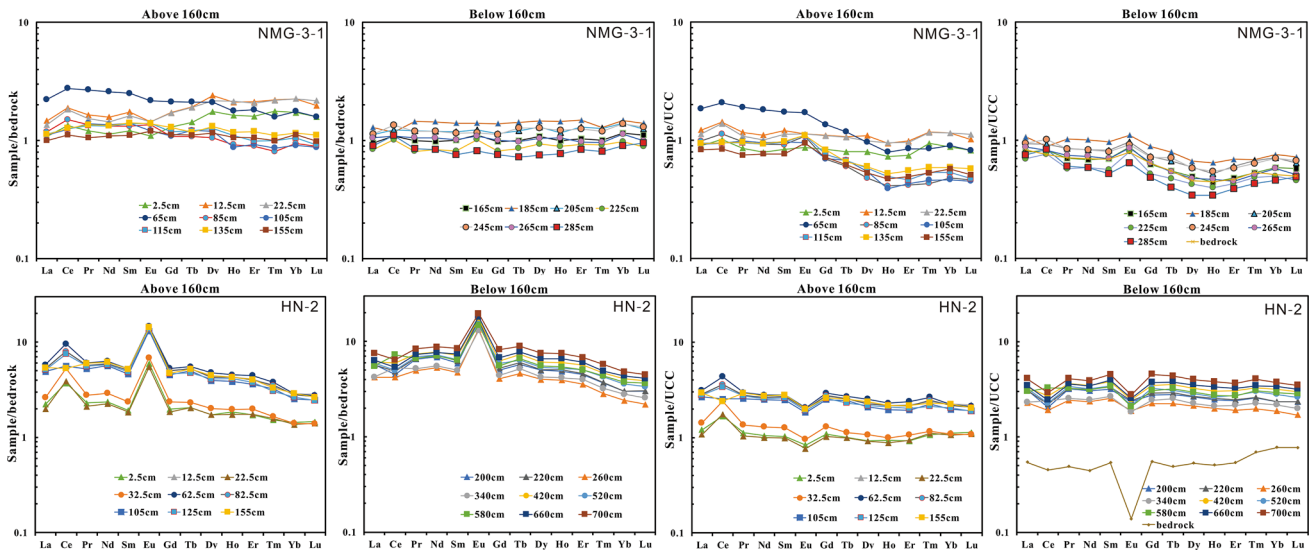

Fig. 1 Distribution patterns of REE normalized to bedrock (granite) and to upper continental crust (UCC)

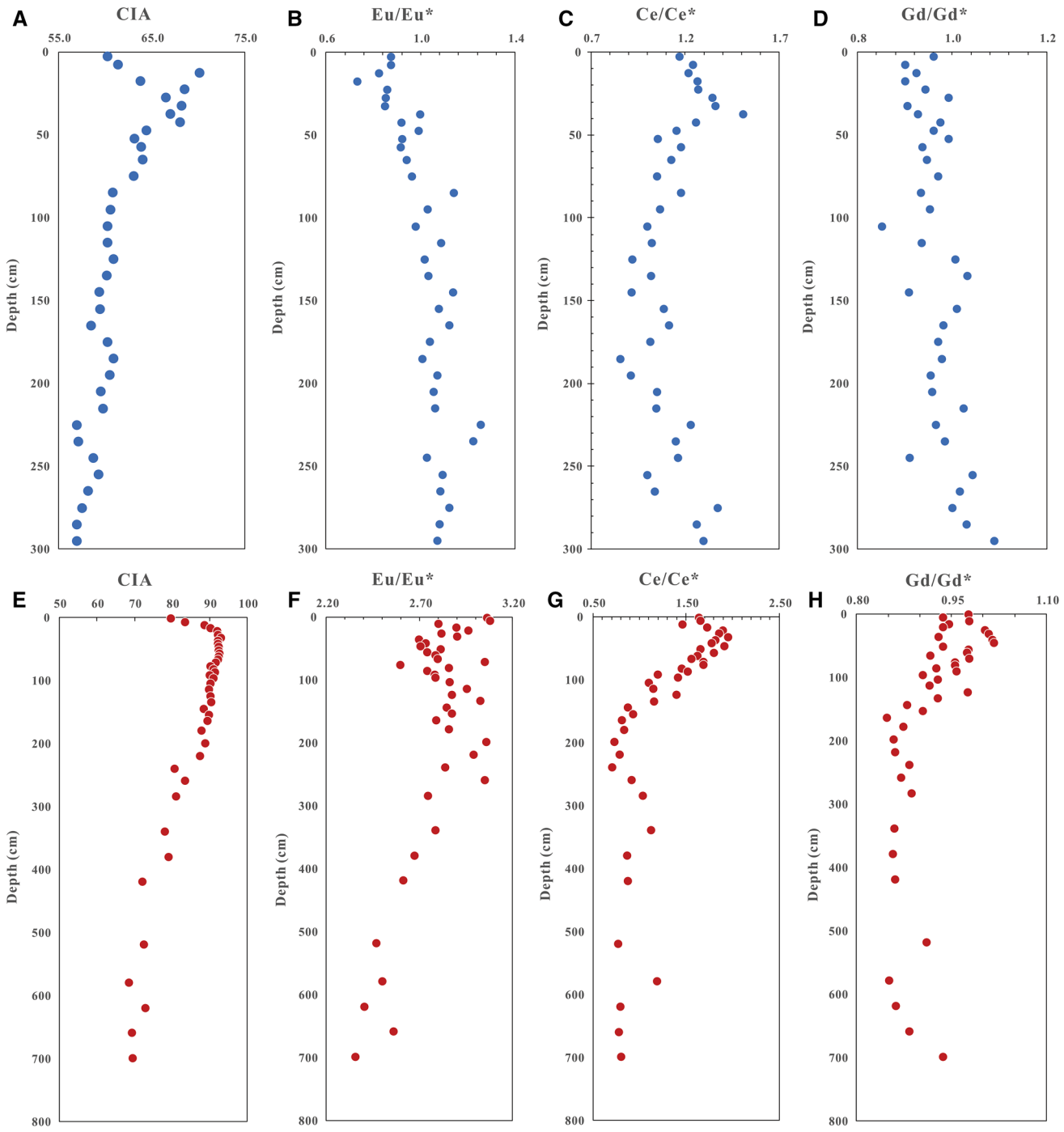

Fig. 2 **a–d** Profile of NMG-3-1, **e–h** profile of HN-2. All the anomalies are normalized to bedrock

4 Discussion and conclusions

The profile NMG-3-1 is in the incipient stage of weathering; hence, REEs of most samples were similar to those of bedrock. Only the upper layer of NMG-3-1 was slightly enriched in REEs (Fig. 1). This REE distribution pattern is consistent with CIA values that cluster around 60. However, stronger weathering in the upper layer has not led to significant LREE/HREE fractionation (La_N/Yb_N of 0.9). Aside from top soil samples, the upper layer of the profile showed a slight HREE depletion. In contrast, the profiles in the Strengbach catchment, where mean annual temperature and precipitation are 6 °C and 1400 mm, respectively, exhibit a HREE depletion that increases with depth. The higher temperature and precipitation of Strengbach may increase HREE depletion; however, dissolution of primary

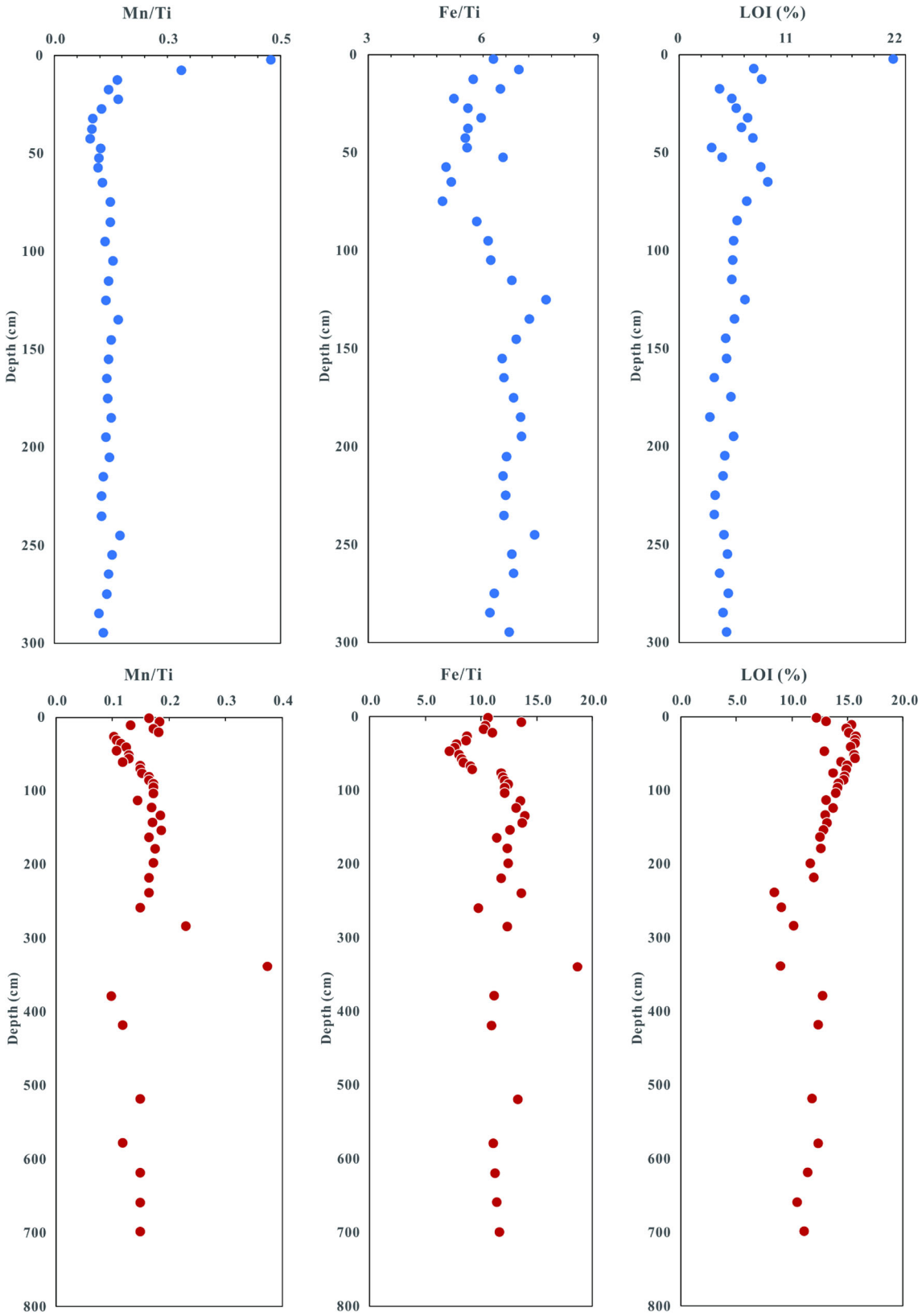

Fig. 3 The Fe/Ti, Mn/Ti, and LOI from the profile NGM-3-1 and HN-2. The *blue dots* and *red dots* denote profile NMG-3-1 and HN-2, respectively

minerals may be still the main process during this stage of weathering in all the profiles.

REEs in profile HN-2 were significantly enriched, consistent with the advanced weathering of the profile, and implying that adsorption on clays, Fe- and Mn-oxides, and organic matter may be the major process. Moreover, stronger enrichment of REE in the lower profile can be attributed to the accumulation of REEs in the illuvial horizon. However, the upper profile (from 30 to 200 cm) showed a slight enrichment of LREEs ($La_N/Yb_N > 1.8$), which is consistent with LREEs' higher adsorption capacity. The Cheras profiles in Malaysia show a similar pattern, controlled by adsorption on clay minerals (Yusoff et al. 2013). In Hunan and Jiangxi profiles under similar climate, LREE/HREE fractionation shows a different pattern, due to the influence of pH on adsorption on clay minerals (Bao and Zhao 2008).

Eu/Eu* values were negatively correlated with CIA in NMG-3-1, whereas the variations in Eu anomaly were positively correlated with CIA in HN-2. The slightly negative Eu anomaly in profile NMG-3-1 was attributed to the slow dissolution of feldspar enriched in Eu (relative to other REEs) (Aubert et al. 2001) and a negative correlation of CIA with Eu/Eu* was previously observed in a basalt profile (Babechuk et al. 2014). In contrast, the positive Eu anomaly (normalized to bedrock) in HN-2 is inconsistent with dissolution of plagioclase. The negative Eu anomalies (normalized to UCC) of soils and intense depletion of Eu in bedrock indicate that external sources contribute to the soils. Furthermore, positive Eu anomalies have been observed in granitic and rhyolitic regolith (Aubert et al. 2001; Bao and Zhao 2008; Brioschi et al. 2013; Vazquez-Ortega et al. 2015), and attributed to dust deposition and vegetation cycle. Given that the profile is covered by dense vegetation and near the shore, dust and litterfall probably caused the positive Eu anomaly in HN-2.

Ce fractionation is strongly influenced by oxidation–reduction reactions in regolith. Generally, Ce(III) can be oxidized to Ce(IV) leading to precipitation of cerianite, generating a positive Ce anomaly. In profile NMG-3-1, there was no obvious correlation between CIA and Ce/Ce*. The slightly positive Ce anomalies and lack of correlation with Mn and Fe (Figs. 2, 3) suggest weak oxidation of Ce and slight coprecipitation by Fe- and Mn-oxides, consistent with the profile's being in the early stage of weathering. In profile HN-2, Ce anomalies increased with decreasing depth (from 250 to 20 cm). Positive Ce anomalies exist in the upper layer of both profiles (Babechuk et al. 2014; Bao and Zhao 2008; Vazquez-Ortega et al. 2015; Yusoff et al. 2013). Moreover, Ce/Ce* showed positive correlation with CIA ($r = 0.78$, $p < 0.01$), indicating Ce anomalies were related to increased weathering. Generally, Ce has similar redox characteristics to Mn, and oxidation of Ce can be coprecipitated with Fe-and Mn-oxides; thus, Mn oxides are associated with a positive Ce anomaly. There is, however, no apparent correlation between Ce/Ce* and Mn/Ti or Fe/Ti (Fig. 3), which can be attributed to higher adsorption of amorphous Fe–Mn-oxides over crystalline ones (Laveuf and Cornu 2009). Furthermore, the clear positive correlation between Ce anomalies and LOI ($r = 0.7$, $p < 0.01$) (above 200 cm) may suggest organic matter also adsorbs Ce. Little is known about the origin of the Gd anomaly. A possible explanation is that organic matter preferentially releases Gd over neighbor REEs during oxidation and decomposition, resulting in a positive Gd anomaly (Ma et al. 2007). In profile HN-2, the strong correlation between Gd/Gd* and Ce/Ce* ($r = 0.8$, $p < 0.01$) (Figs. 2d–h) suggests that Gd and Ce complexed with organic matter derived from decomposed litterfall, then transferred downward with organic ligands, and finally precipitated at the oxic front. Fertilizer does not display clear Gd anomalies (Aubert et al. 2002; Möller et al. 2014), indicating that human activity may not be responsible for the Gd anomalies in profile HN-2.

Acknowledgments This work was jointly supported by the National Natural Science Foundation of China (Grant No. 41210004; 41661144042) and National Basic Research Program (973 project) of China (2013CB956401).

References

Aubert D, Stille P, Probst A (2001) REE fractionation during granite weathering and removal by waters and suspended loads: Sr and Nd isotopic evidence. Geochim Cosmochim Acta 65:387–406. doi:10.1016/S0016-7037(00)00546-9

Aubert D, Stille P, Probst A, Gauthier-lafaye F, Pourcelot L, Del Nero M (2002) Characterization and migration of atmospheric REE in soils and surface waters. Geochim Cosmochim Acta 66:3339–3350. doi:10.1016/S0016-7037(02)00913-4

Babechuk MG, Widdowson M, Kamber BS (2014) Quantifying chemical weathering intensity and trace element release from two contrasting basalt profiles, Deccan Traps, India. Chem Geol 363:56–75. doi:10.1016/j.chemgeo.2013.10.027

Bao ZW, Zhao ZH (2008) Geochemistry of mineralization with exchangeable REY in the weathering crusts of granitic rocks in South China. Ore Geol Rev 33:519–535. doi:10.1016/j.oregeorev.2007.03.005

Brioschi L, Steinmann M, Lucot E, Pierret MC, Stille P, Prunier J, Badot PM (2013) Transfer of rare earth elements (REE) from natural soil to plant systems: implications for the environmental availability of anthropogenic REE. Plant Soil 366:143–163. doi:10.1007/s11104-012-1407-0

Henderson P (1984) General geochemical properties and abundances of the rare earth elements. In: Henderson P (ed) Rare earth element geochemistry: developments in geochemistry, vol 2. Elsevier Science Publishers, Amsterdam

Laveuf C, Cornu S (2009) A review on the potentiality of rare earth elements to trace pedogenetic processes. Geoderma 154:1–12. doi:10.1016/j.geoderma.2009.10.002

Ma J-L, Wei G-J, Xu Y-G, Long W-G, Sun W-D (2007) Mobilization and re-distribution of major and trace elements during extreme

weathering of basalt in Hainan Island, South China. Geochim Cosmochim Acta 71:3223–3237. doi:10.1016/j.gca.2007.03.035

Möller P, Knappe A, Dulski P (2014) Seasonal variations of rare earths and yttrium distribution in the lowland Havel River, Germany, by agricultural fertilization and effluents of sewage treatment plants. Appl Geochem 41:62–72. doi:10.1016/j.apgeochem.2013.11.011

Rudnick RL, Gao S (2003) Composition of the continental crust. In: Holland HD, Turekian KK (eds) Treatise on geochemistry, vol 3. Pergamon, Oxford, pp 1–64. doi:10.1016/B0-08-043751-6/03016-4

Vazquez-Ortega A, Perdrial J, Harpold A, Zapata-Rios X, Rasmussen C, McIntosh J, Schaap M, Pelletier JD, Brooks PD, Amistadi MK, Chorover J (2015) Rare earth elements as reactive tracers of biogeochemical weathering in forested rhyolitic terrain. Chem Geol 391:19–32. doi:10.1016/j.chemgeo.2014.10.016

Vermeire M-L, Cornu S, Fekiacova Z, Detienne M, Delvaux B, Cornélis J-T (2016) Rare earth elements dynamics along pedogenesis in a chronosequence of podzolic soils. Chem Geol 446:163–174. doi:10.1016/j.chemgeo.2016.06.008

Yusoff ZM, Ngwenya BT, Parsons I (2013) Mobility and fractionation of REEs during deep weathering of geochemically contrasting granites in a tropical setting, Malaysia. Chem Geol 349–350:71–86. doi:10.1016/j.chemgeo.2013.04.016